Investigating the corrosion inhibitory properties of 1-benzyl-4-imidazolidinone on mild steel in hydrochloric acid: a thorough experimental and quantum chemical study

M.H. Abdulkareem,[1] Z.A. Gbashi,[1] B.A. Abdulhussein,[2] M.M. Hanoon,[1] A.A.H. Kadhum,[3] A.A. Alamiery[4,5]* and W.K. Al-Azzawi[6]

[1]Department of Production Engineering and Metallurgy, University of Technology, Baghdad, 10001, Iraq
[2]Chemical Engineering Department, University of Technology, Baghdad, 10001, Iraq
[3]University of Al-Ameed, Karbala, 56001, Iraq
[4]Faculty of Engineering and Built Environment, Universiti Kebangsaan Malaysia, Bangi, Selangor 43600, Malaysia
[5]Energy and Renewable energies Center, University of Technology, Baghdad, 10001, Iraq
[6]Al-Farahidi University, Baghdad, 10001, Iraq
**E-mail: dr.ahmed1975@gmail.com*

Abstract

This study investigates the inhibitory efficacy of 1-benzyl-4-imidazolidinone (BMI) in a 1 M hydrochloric acid (HCl) solution as a corrosion inhibitor for mild steel in aggressive environments. Varying the inhibitor concentration reveals notable inhibition efficiency, reaching 94.8% at 0.5 mM BMI in 1 M HCl. The research explores the impact of immersion periods and temperatures on BMI's inhibitory performance. Integrating experimental weight loss measurements with density functional theory (DFT) quantum chemical computations, the study uncovers the inhibitory mechanism. Experimental results demonstrate a significant reduction in the corrosion rate of mild steel with BMI, highlighting its potential as a highly efficient corrosion inhibitor. DFT calculations attribute BMI's inhibitory action to robust adsorption onto the mild steel surface, aligning with the Langmuir adsorption isotherm and suggesting the formation of a protective monolayer. This monolayer acts as a potent barrier, impeding access to active sites and retarding the corrosion process, contributing to the observed high inhibition efficiency. In conclusion, the research underscores BMI's remarkable inhibition efficiency in 1 M HCl for mild steel, considering varying inhibitor concentrations, immersion periods, and temperatures. Insights from experimental and theoretical approaches emphasize BMI's potential as an effective corrosion inhibitor, offering valuable contributions to practical corrosion protection methods, particularly beneficial for industries relying on mild steel components in corrosive environments.

Received: August 5, 2023. Published: February 27, 2024 doi: 10.17675/2305-6894-2024-13-1-21

Keywords: *corrosion inhibitor, BMI, inhibition efficiency, hydrochloric acid, quantum chemical calculations.*

1. Introduction

Corrosion is an ever-present challenge in various industries, where metal structures and components are subjected to aggressive environments. The deterioration of metals due to chemical or electrochemical reactions with their surroundings is known as the corrosion process [1–3]. Among different types of metals, mild steel is widely used in industries due to its favorable mechanical properties and cost-effectiveness. However, mild steel is highly susceptible to corrosion, leading to significant economic losses and safety concerns. Industries such as petrochemical, manufacturing, construction, and transportation heavily rely on mild steel for various applications, including pipelines, storage tanks, bridges, and machinery [4, 5]. The durability and reliability of these industrial assets are compromised by the corrosive attack, necessitating effective corrosion protection strategies. Hydrochloric acid (HCl) solution is commonly used in industries for various purposes, such as pickling and cleaning metal surfaces, pH adjustment, and chemical synthesis [6, 7]. However, its aggressive nature makes it a potent corrosive agent, posing a significant challenge for the protection of mild steel components that come into contact with HCl solutions. Therefore, the development of efficient corrosion inhibitors is of paramount importance to mitigate the detrimental effects of HCl on mild steel [8].

Organic corrosion inhibitors have emerged as indispensable agents for safeguarding metal structures and components from the deleterious effects of corrosion. Their versatile chemical structures and tunable properties make them suitable for a broad spectrum of industrial applications [9–11]. These inhibitors work by forming a protective barrier on the metal surface, impeding the electrochemical reactions that drive the corrosion process. One significant advantage of organic inhibitors is their potential for tailoring their molecular structures to enhance their inhibitory efficiency for specific metals and corrosive environments. The incorporation of nitrogen and oxygen atoms in the structure of organic corrosion inhibitors plays a pivotal role in enhancing their inhibitory performance [12–14]. Nitrogen-containing heterocyclic compounds, such as imidazole, benzimidazole, and triazole derivatives, have garnered particular attention due to the presence of nitrogen atoms in their five-membered rings [15–17]. These heterocyclic rings facilitate the formation of coordinate bonds with metal cations, leading to the adsorption of the inhibitor molecules on the metal surface. This adsorption process involves the donation of lone pairs of electrons from the nitrogen atoms to the metal ions, resulting in the formation of a protective film. Similarly, the introduction of oxygen atoms, as seen in oxadiazole derivatives, further enhances the inhibitory properties of organic corrosion inhibitors [18]. Oxygen atoms in the heterocyclic rings can form coordination complexes with metal centers, leading to strong adsorption on the metal surface. The presence of oxygen atoms can also facilitate hydrogen bonding interactions, allowing for the formation of stable inhibitor-metal complexes [19].

The strategic placement of nitrogen and oxygen atoms within the organic inhibitor molecules contributes to their ability to coordinate with metal surfaces and create a barrier against aggressive ions and corrosive species. This protective film effectively shields the

metal surface from further corrosive attack, thereby retarding the corrosion process. The uses of organic corrosion inhibitors are extensive and diverse. They find application in various industries, such as oil and gas, petrochemical, automotive, and marine, where metal components are exposed to corrosive environments [20]. Organic inhibitors are employed for the protection of pipelines, storage tanks, heat exchangers, boilers, and other critical equipment, ensuring their longevity and performance. Furthermore, the eco-friendly nature of organic inhibitors, compared to traditional inorganic inhibitors, makes them increasingly attractive for sustainable corrosion protection strategies. Their biodegradability and lower environmental impact align with the growing emphasis on green and environmentally conscious practices in industry [21].

Organic inhibitors derived from imidazole have garnered significant attention in corrosion inhibition studies due to their versatile structures and favorable inhibitory properties. Imidazole, with its five-membered ring containing two nitrogen atoms, serves as a valuable precursor for synthesizing various imidazole derivatives. These derivatives can be fine-tuned to impart specific inhibitory characteristics, making them effective candidates for corrosion protection in different industrial applications. Some notable examples of organic inhibitors derived from imidazole are highlighted below [22–25]:

1. Benzimidazole derivatives: benzimidazole, a fused imidazole derivative, has been extensively studied for its corrosion inhibition capabilities. Various benzimidazole derivatives, such as 2-mercaptobenzimidazole, 2-aminobenzimidazole, and *N*-phenylbenzimidazole, have shown excellent inhibition efficiency for metals in aggressive environments.
2. Triazole derivatives: triazole is another heterocyclic compound structurally related to imidazole, and its derivatives have shown promising inhibitory effects. For instance, 1,2,4-triazole and 1,2,3-triazole derivatives have demonstrated substantial corrosion inhibition for metals exposed to acidic solutions.
3. Imidazoline derivatives: imidazoline compounds, derived from imidazole, have been widely employed as corrosion inhibitors for carbon steel in various corrosive media, including acidic and alkaline solutions. Examples include 2-heptadecyl-1,3-dimethylimidazoline and 2-dodecyl-1,3-dimethylimidazoline.
4. Pyrazole derivatives: pyrazole, a nitrogen-containing heterocycle similar to imidazole, has inspired the synthesis of effective corrosion inhibitors. Pyrazole derivatives, such as 3,5-dimethylpyrazole and 4-hydroxy-1-methylpyrazole, have demonstrated appreciable corrosion inhibition for metals in acidic and neutral solutions.
5. Oxadiazole derivatives: oxadiazole is a five-membered ring compound containing nitrogen and oxygen atoms and has been utilized to develop potent corrosion inhibitors.

6. Various oxadiazole derivatives, such as 2,5-dihydroxy-1,3,4-oxadiazole and 2-mercapto-1,3,4-oxadiazole, have shown remarkable inhibitory effects on metal corrosion.

These examples represent only a fraction of the diverse array of organic inhibitors derived from imidazole. The chemical modification and functionalization of the imidazole core enable researchers to tailor the inhibitory properties of these compounds, optimizing their performance for specific metal-substrate and corrosive environments. As the understanding of the structure-activity relationship of imidazole-based inhibitors continues to advance, the potential for developing efficient and eco-friendly corrosion inhibitors for a wide range of industrial applications grows substantially.

The primary aim of this research is to assess the corrosion inhibition efficiency (IE%) of BMI at an inhibitor concentration of 0.5 mM in 1 M HCl solution. The study seeks to evaluate the extent to which the inhibitor can effectively protect mild steel from corrosive attack. Additionally, the inhibitory mechanism will be explored to unravel the interactions between BMI and the mild steel surface. By employing a combined approach of experimental and theoretical techniques, this work endeavors to gain insights into the adsorption behavior of BMI onto the metal surface. The Langmuir adsorption isotherm will be utilized to elucidate the formation of a monolayer, which contributes to the inhibition process. The obtained synergistic insights will provide a deeper understanding of the corrosion inhibition mechanism, shedding light on the potential practical applications of BMI (Figure 1) as an efficient and eco-friendly corrosion inhibitor for mild steel in acidic environments. In conclusion, the significance of this research lies in its contribution to the advancement of corrosion protection strategies in industries where mild steel is frequently exposed to hydrochloric acid solutions. The findings have the potential to pave the way for the development of novel corrosion inhibitors, enhancing the durability and reliability of metal structures and components, and thereby reducing economic losses and ensuring safety in industrial applications.

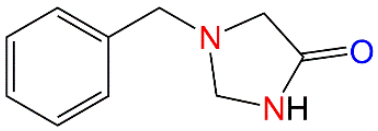

Figure 1. The structure of BMI.

2. Experimental Methodology

2.1. Materials and reagents

All the materials and reagents utilized in this study were obtained from Sigma-Aldrich/Malaysia, ensuring high-quality and consistent results. To create the corrosive medium for the experiments, a 1 M hydrochloric acid (HCl) solution was prepared by diluting analytical grade 37% HCl solution with double-distilled water. Inhibitor

concentrations ranging from 0.1 to 1.0 mM were achieved by diluting the inhibitor in the 1 M HCl solution [26].

2.2. Sample preparation

The mild steel samples used in this study underwent thorough analysis for their chemical composition using X-ray fluorescence spectrometry. Following the ASTM G1-03 protocol, the samples were prepared and polished using silicon carbide series plates. Before immersion, the mild steel coupons were meticulously cleaned with double-distilled water and acetone, ensuring the removal of any contaminants, and then dried in an oven [27].

2.3. Weight loss measurements

The weight loss measurements were performed by immersing the mild steel samples in 500 ml glass beakers containing 400 ml of the prepared 1 M HCl solution with varying concentrations of the inhibitor. The experiments were carried out at a temperature of 303 K using a water bath, adhering to the NACE TM0169/G31 protocol [28]. The samples were exposed for different time periods (1, 5, 10, 24 and 48 hours), and the corrosion products were meticulously wiped off the surface before the coupons were dried and weighed. The difference in weight was recorded, and the mass variation at the estimated time, along with the original mass of the metallic sample, represented the weight loss achieved. The mild steel coupons were immersed in corrosive media (1 M HCl) containing different inhibitor concentrations (0.1, 0.2, 0.3, 0.4, 0.5 and 1 mM) at temperatures of 303, 313, 323 and 333 K using a water bath to examine the effect of temperature [27, 28]. The average rate of corrosion was calculated after being exposed in triplicate, and the rate of corrosion and inhibition efficiency were determined using the following equations (1, 2):

$$C_{\mathrm{R}} = \frac{W}{a \cdot d \cdot t} \tag{1}$$

$$IE\% = \left[1 - \frac{C_{\mathrm{R(i)}}}{C_{\mathrm{R}_0}}\right] \cdot 100 \tag{2}$$

where W is the weight loss (mg) of the sample, a is the surface area of mild steel (cm^2), d is the density of the mild steel coupon (g/cm^3), and t is the exposure time (h). The corrosion rates in the absence and presence of the inhibitor were denoted as C_{R_0} and $C_{\mathrm{R(i)}}$, respectively.

The coverage area (θ) for both uninhibited and inhibited solutions was determined using the following equation (3):

$$\theta = 1 - \frac{C_{\mathrm{R(i)}}}{C_{\mathrm{R}_0}} \tag{3}$$

2.4. DFT calculations

Density Functional Theory (DFT) calculations were conducted using the Gaussian 09 software to investigate the molecular interactions between the inhibitor and the metal surface. The optimization of the inhibitor's structure in the gaseous state was accomplished using the B3LYP method and the basis set "6-31G++(d,p)". By employing Koopmans theory, the ionization potential (*I*) and electron affinity (*A*) were determined based on the highest occupied molecular orbital (E_{HOMO}) and the lowest unoccupied molecular orbital (E_{LUMO}), respectively. The following equations (4, 5) were employed for calculating *I* and *A* [29, 30]:

$$I = -E_{HOMO} \tag{4}$$

$$A = -E_{LUMO} \tag{5}$$

The electronegativity (χ), hardness (η), and softness (σ) values were calculated using the following equations (6–8):

$$\chi = \frac{I + A}{2} \tag{6}$$

$$\eta = \frac{I - A}{2} \tag{7}$$

$$\sigma = \frac{1}{\eta} \tag{8}$$

Furthermore, the number of electrons transferred (Δ*N*) was determined using Equation 9 [30]. The electronegativity value of iron was established as 7 eV, with a hardness value of zero eV. Based on these results, Equation 10 was formulated.

$$\Delta N = \frac{\chi_{Fe} - \chi_{inh}}{2(\eta_{Fe} + \eta_{inh})} \tag{9}$$

$$\Delta N = \frac{7 - \chi_{inh}}{2 \cdot \eta_{inh}} \tag{10}$$

2.5. Adsorption isotherm studies

To gain comprehensive insights into the properties of the studied molecules, various types of adsorption isotherms, including Frumkin, Temkin, and Langmuir, were employed. These isotherms aid in determining the extent of inhibitor coverage on the metal surface. Weight loss measurements were conducted to assess the surface coverage of the inhibitor at various concentrations in corrosive media [31]. The detailed experimental methodology presented above outlines the rigorous procedures employed to evaluate the effectiveness of the organic corrosion inhibitor BMI for mild steel in hydrochloric acid solution. The combination of weight loss measurements, DFT calculations, and adsorption isotherm studies offers

valuable insights into the inhibition efficiency and inhibitory mechanisms, providing a solid foundation for practical industrial applications.

3. Results and Discussion

3.1. Weight loss measurements

3.1.1. Effect of inhibitor concentrations

In order to evaluate the impact of inhibitor concentrations on the corrosion inhibition of mild steel in a 1 M HCl solution, weight loss measurements were conducted. The mild steel samples were immersed in the corrosive medium for a duration of 5 hours, and varying concentrations of the inhibitor, ranging from 0.1 to 1.0 mM, were introduced into the solution. Figure 2 illustrates the corrosion rate and inhibition effectiveness as a function of different inhibitor concentrations [32, 33].

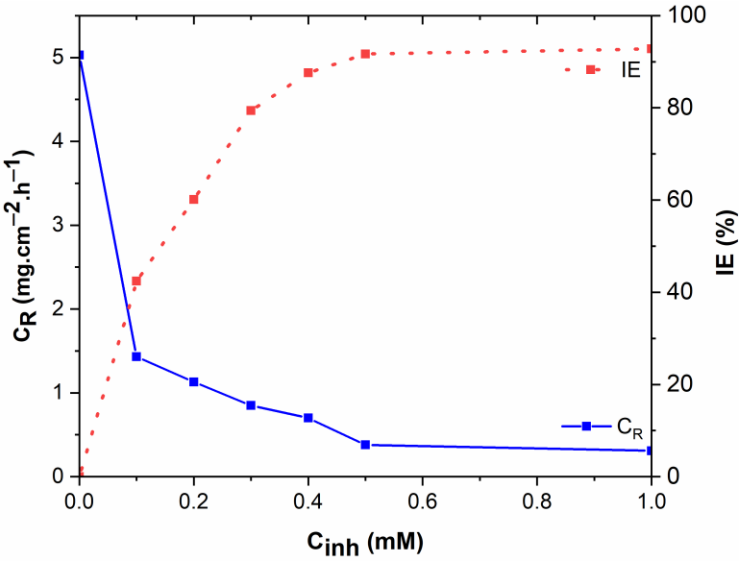

Figure 2. Corrosion rate and inhibition effectiveness at varying inhibitor concentrations.

As depicted in Figure 2, the corrosion rate of mild steel significantly decreases with increasing inhibitor concentration. This reduction in corrosion rate is attributed to the adsorption of the BMI inhibitor onto the mild steel surface, forming a protective layer that hinders aggressive ions' access to the metal surface. The adsorption of the inhibitor molecules is believed to occur through coordination bonds between the nitrogen atoms in the inhibitor's imidazole ring and the metal cations, creating a stable and compact protective film. Furthermore, the inhibition effectiveness, as calculated from the weight loss measurements, demonstrates a substantial improvement as the inhibitor concentration is increased [34]. At a low inhibitor concentration of 0.1 mM, the inhibition effectiveness shows a moderate level of protection. However, as the inhibitor concentration rises to 0.5 mM and beyond, the inhibition effectiveness reaches its peak, showing a remarkable corrosion inhibition of mild steel [35, 36]. The observed trend in inhibition effectiveness

corroborates the Langmuir adsorption isotherm behavior, where the inhibitor molecules form a monolayer on the metal surface, leading to a saturation point beyond which further increase in concentration does not significantly impact the inhibition effectiveness. This behavior indicates the formation of a complete and dense protective layer, preventing additional inhibitor molecules from adsorbing and making the corrosion rate nearly negligible. The results highlight the crucial role of inhibitor concentration in determining the corrosion inhibition efficiency of BMI for mild steel in a 1 M HCl solution. Higher inhibitor concentrations lead to stronger adsorption and more extensive surface coverage, resulting in better corrosion protection [37]. Therefore, optimizing the inhibitor concentration is essential to achieving the desired level of corrosion inhibition in practical applications. The significant inhibition effectiveness of BMI at a concentration of 0.5 mM suggests its potential as an efficient and cost-effective corrosion inhibitor for mild steel in acidic environments. The findings from this study provide valuable insights for the development of practical corrosion protection strategies and pave the way for further exploration of this compound's applicability in industrial settings [38, 39].

3.1.2. Effect of immersion time

To investigate the influence of immersion time on the corrosion inhibition of mild steel in a 1 M HCl solution, weight loss measurements were carried out. The mild steel samples were immersed in the corrosive medium for different time periods of 1, 5, 10, 24 and 48 hours. These experiments were performed at a constant temperature of 303 K, and varying concentrations of the inhibitor (ranging from 0.1 to 1.0 mM) were introduced into the solution. Figure 3 illustrates the corrosion rate and inhibition effectiveness at different immersion times and various inhibitor concentrations at 303 K [40, 41].

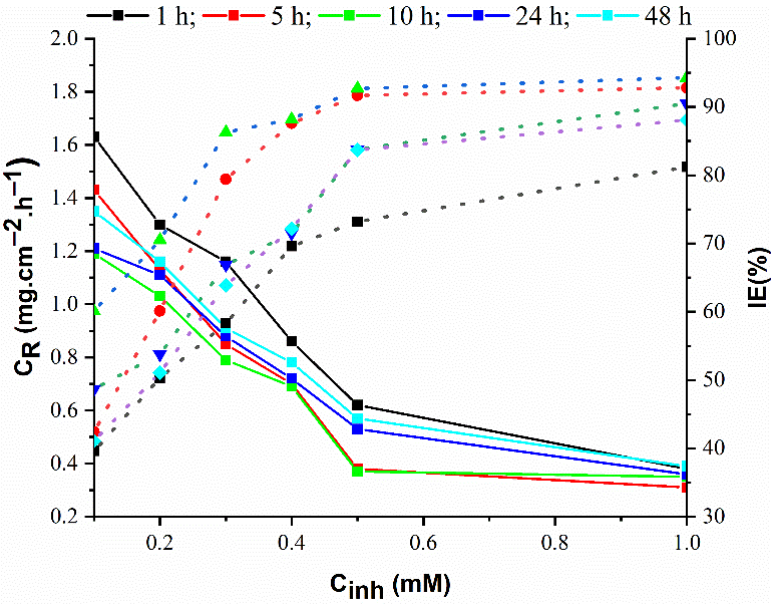

Figure 3. Corrosion rate and inhibition effectiveness at different immersion times and various inhibitor concentrations (303 K).

As shown in Figure 3, the inhibition efficiency at all inhibitor concentrations exhibits an overall increasing trend with an increase in immersion time from 1 hour to 10 hours. This suggests that the protective film formed by BMI on the mild steel surface becomes more stable and effective in hindering corrosive attacks over this time range. The inhibitor molecules gradually adsorb and rearrange on the metal surface, leading to improved surface coverage and reduced access of aggressive ions to the metal. However, an interesting observation is seen at 24 hours of immersion time, where the inhibition efficiency starts to exhibit a slight decrease [42, 43]. This phenomenon could be attributed to several factors. First, the protective film formed by the inhibitor might undergo partial desorption or restructuring due to prolonged exposure to the corrosive environment. Additionally, the accumulation of corrosion products on the metal surface may hinder further inhibitor adsorption, leading to a slight decline in inhibition efficiency. The overall trend suggests that there exists an optimal immersion time (around 10 hours) during which the inhibitor exhibits the highest corrosion inhibition effectiveness. Beyond this time point, the inhibitor's efficiency may start to plateau or slightly decline due to the aforementioned factors [44, 45].

Furthermore, it is important to note that at all inhibitor concentrations, BMI demonstrates its ability to significantly reduce the corrosion rate of mild steel over the studied immersion times. The increase in inhibition efficiency up to 10 hours underscores the compound's potential as a reliable corrosion inhibitor for extended exposure periods. In conclusion, the effect of immersion time on the corrosion inhibition of mild steel in a 1 M HCl solution was investigated through weight loss measurements [46, 47]. The results indicate that the inhibition efficiency of BMI increases with increasing immersion time up to 10 hours, after which a slight decline is observed at 24 hours. This finding highlights the importance of considering the immersion time when evaluating the performance of the inhibitor in practical applications. The understanding of these dynamics provides valuable insights for optimizing the usage of this compound as an effective corrosion inhibitor for mild steel in acidic environments over extended exposure periods.

3.1.3. Effect of temperature

The influence of temperature on the corrosion inhibition of mild steel in a 1 M HCl solution was investigated using weight loss measurements. The mild steel samples were immersed in the corrosive medium for a fixed duration of 5 hours. The experiments were conducted at different temperatures, namely 303, 313, 323 and 333 K. Varying concentrations of the inhibitor (ranging from 0.1 to 1.0 mM) were introduced into the solution. Figure 4 illustrates the corrosion rate and inhibition effectiveness for the 5-hour immersion period at different temperatures and various inhibitor concentrations [48].

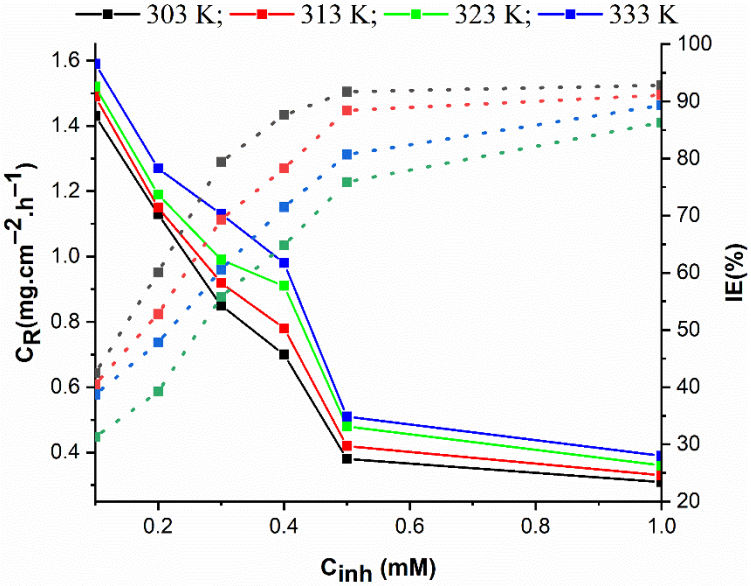

Figure 4. Corrosion rate and inhibition effectiveness at different temperatures and various inhibitor concentrations (5-hour immersion period).

As shown in Figure 4, the corrosion rate of mild steel tends to slightly increase with rising temperature at all inhibitor concentrations. This observation aligns with the well-known principle that higher temperatures generally accelerate the rate of corrosion reactions. The increased kinetic energy of the corrosive species at elevated temperatures enhances their interaction with the metal surface, leading to a higher corrosion rate. Additionally, the inhibition efficiency of BMI at all inhibitor concentrations demonstrates a decreasing trend with increasing temperature [49, 50]. As the temperature rises, the thermal energy favors the breaking of weak bonds between the inhibitor molecules and the metal surface, thus reducing the stability of the protective film formed by the inhibitor. This weakening of the adsorption forces results in a less effective inhibition of the corrosion process. Despite the decrease in inhibition efficiency with increasing temperature, it is essential to note that BMI remains effective in reducing the corrosion rate of mild steel even at elevated temperatures. The compound continues to provide significant corrosion protection, albeit at a slightly reduced level compared to lower temperatures. To further optimize the application of BMI as a corrosion inhibitor for mild steel in acidic environments, it is important to consider the operating temperature. Lower temperatures are generally more favorable for achieving higher inhibition efficiencies due to the enhanced stability of the inhibitor film. However, even at higher temperatures, the compound exhibits considerable corrosion inhibition, indicating its potential applicability in a wide range of temperature conditions. In conclusion, the effect of temperature on the corrosion inhibition of mild steel in a 1 M HCl solution was investigated through weight loss measurements. The results reveal that the corrosion rate of mild steel slightly increases with rising temperature at all inhibitor concentrations. Moreover, the inhibition efficiency of BMI demonstrates a decreasing trend with increasing temperature, although it continues to provide significant corrosion protection. The

understanding of these temperature-dependent dynamics is vital for optimizing the application of this compound as a corrosion inhibitor in various industrial scenarios, especially when considering varying temperature conditions.

3.2. Effect of adsorption isotherm analysis

To gain deeper insights into the adsorption behavior of BMI inhibitor on the mild steel surface, adsorption isotherm analysis was performed, with a focus on the Langmuir isotherm model. Figure 5 illustrates the fitting of the Langmuir isotherm to the experimental data, and the analysis provides valuable information regarding the adsorption mechanism and the nature of bonding between the inhibitor molecules and the metal surface.

The Langmuir isotherm equation is expressed as follows:

$$\frac{C_{\text{inh}}}{\theta} = K_{\text{ads}}^{-1} + C \tag{11}$$

where C_{inh} is the inhibitor concentration, θ is the surface coverage, K_{ads} is the constant of adsorption, and C is the equilibrium concentration of the inhibitor.

The fitting of the Langmuir isotherm to the experimental data, as depicted in Figure 5, demonstrates a good fit with a regression coefficient (R^2) value of 0.98844. The high R^2 value close to 1 indicates that the Langmuir isotherm accurately describes the adsorption behavior of BMI on the mild steel surface [51, 52]. The slope value of the Langmuir isotherm (0.93±0.05) reflects the relationship between the inhibitor concentration and the surface coverage. The slope indicates that as the inhibitor concentration increases, the surface coverage also increases, indicating a higher extent of inhibitor adsorption onto the metal surface. The intercept value of the Langmuir isotherm (0.11±0.02) has a significant physical significance. It represents the theoretical maximum surface coverage (θ_{max}) when the inhibitor concentration approaches infinity. The value of θ_{max} suggests that the inhibitor molecules form a complete monolayer on the metal surface, effectively blocking the active sites and hindering further corrosion.

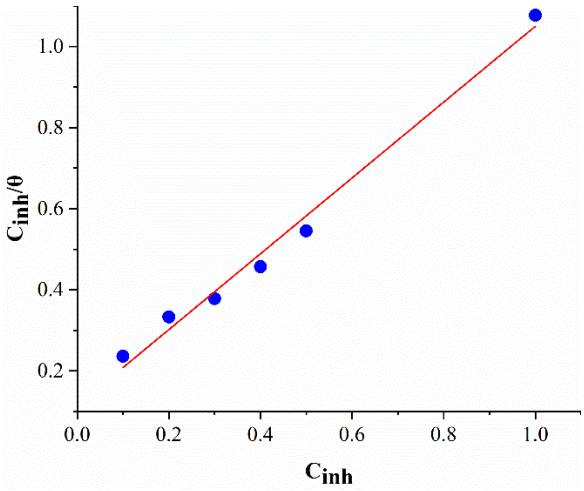

Figure 5. Langmuir adsorption isotherm.

The thermodynamic aspects of the adsorption process were analyzed by calculating the standard free energy of adsorption ΔG_{ads}^{0} using Equation 12:

$$\Delta G_{ads}^{0} = -RT \,\mathrm{Ln}(55{,}5 \cdot K_{ads}) \tag{12}$$

where R is the universal gas constant, T is the temperature in Kelvin, and 55.5 is the molar volume of water.

The calculated ΔG_{ads}^{0} value of –35.68 kJ·mol^{-1} indicates a negative value, suggesting a spontaneous and favorable adsorption process. This negative value indicates that the adsorption of BMI onto the mild steel surface is thermodynamically stable. The negative ΔG_{ads}^{0} value suggests that the adsorption process involves chemisorption, which is a stronger and more permanent bonding mechanism than physisorption. The chemisorption mechanism involves the sharing or transfer of electrons between the inhibitor molecules and the metal surface, leading to strong covalent bonds. The adsorption mechanism of BMI on the mild steel surface may involve various interactions, including between donor and acceptor π-bonds, unoccupied iron d-orbitals, electrostatic interactions, and interactions between unoccupied iron d-orbitals and unpaired electrons of nitrogen atoms. The combination of these mechanisms facilitates the adsorption of the inhibitor onto the metallic surface and provides effective corrosion protection. Overall, the adsorption isotherm analysis using the Langmuir model sheds light on the adsorption behavior and mechanisms of BMI on the mild steel surface. The good fit of the Langmuir isotherm to the experimental data, along with the negative ΔG_{ads}^{0} value, indicates a spontaneous and chemically favorable adsorption process. The understanding of the adsorption behavior and mechanisms is essential for optimizing the use of this inhibitor as an effective corrosion inhibitor for mild steel in aggressive environments.

3.3. DFT

3.3.1. Quantum chemical calculations

Quantum chemical calculations using density functional theory (DFT) at the B3LYP/6-311G (d, p) level were performed to gain further insights into the inhibitory behavior of BMI. The DFT calculations provided valuable electronic structure information, including the highest occupied molecular orbital (HOMO) and lowest unoccupied molecular orbital (LUMO) energies, as well as several other DFT variables that contribute to understanding the inhibitor's corrosion inhibition mechanism. Table 1 summarizes the DFT variables for BMI molecules in the gas phase [30, 53].

Table 1. DFT variables for BMI molecules in gas phase.

ΔE_{HOMO} (eV)	ΔE_{LUMO} (eV)	ΔE (eV)	χ (eV)	η (eV)	σ (eV^{-1})	ΔN (eV)
–9.288	–1.113	8.175	5.701	4.201	0.238	1.750

The optimized structure and frontier molecular orbitals (MOs) of tested inhibitor are presented in Figure 6. The HOMO energy (E_{HOMO}) and LUMO energy (E_{LUMO}) values were found to be –9.288 eV and –1.113 eV, respectively. The energy difference between HOMO and LUMO (ΔE) was calculated to be 8.175 eV. These energy values provide information about the stability and reactivity of the inhibitor [54]. A smaller ΔE value indicates that the inhibitor is more susceptible to undergo chemical reactions, suggesting its reactivity in inhibiting the corrosion process. The electronegativity (χ) of BMI was determined to be 5.701 eV. Electronegativity represents the ability of the inhibitor to attract electrons, and higher values indicate a stronger tendency to form bonds with other atoms or metal surfaces. This suggests that the inhibitor has the potential to interact more effectively with the metal surface, contributing to its inhibition efficiency [55].

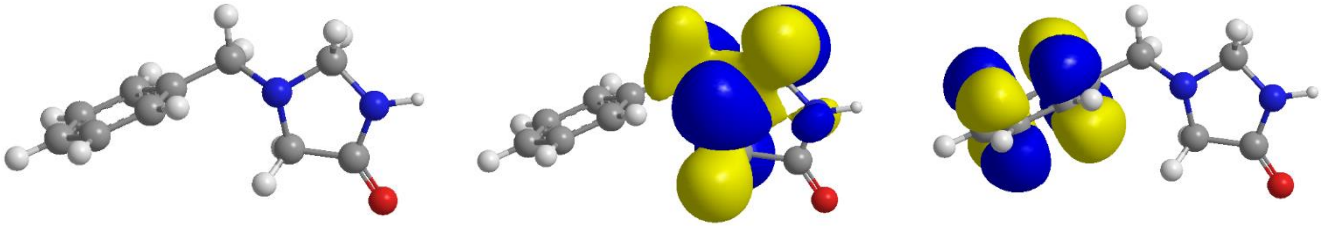

Figure 6. The optimized structure and frontier MOs of tested inhibitor.

The hardness (η) and softness (σ) values were calculated to be 4.201 eV and 0.238 eV^{-1}, respectively. Hardness is a measure of the resistance of the inhibitor to undergo changes in its electron distribution, while softness reflects its ability to accommodate electronic changes. Higher hardness indicates a more stable inhibitor, while higher softness suggests that the inhibitor is more prone to accepting or donating electrons, thus participating in charge transfer processes. Furthermore, the number of electrons transferred (ΔN) was determined to be 1.750 eV. This value represents the extent of charge transfer between the inhibitor and the metal surface [56, 57]. A higher ΔN value indicates a stronger interaction between the inhibitor and the metal, implying a more effective inhibition of the corrosion process. The DFT variables provide a comprehensive understanding of the electronic properties and reactivity of BMI. The negative HOMO energy indicates that the inhibitor can act as an electron donor, forming stable bonds with metal atoms on the surface of mild steel. Conversely, the LUMO energy being negative also implies that the inhibitor can accept electrons, facilitating the formation of coordination bonds with metal ions [58–60]. Overall, the quantum chemical calculations based on DFT have provided valuable electronic structure information, shedding light on the inhibitory behavior of BMI. The calculated HOMO and LUMO energies, as well as the electronegativity, hardness, softness, and number of transferred electrons, offer crucial insights into the interactions between the inhibitor and the metal surface, providing a theoretical foundation for the observed corrosion inhibition efficiency [61–64]. The combined experimental and theoretical approach contributes to a

comprehensive understanding of the inhibitory mechanism of BMI, supporting its potential application as a corrosion inhibitor for mild steel in aggressive environments.

3.3.2. Atomic charges

The quantum chemical calculations based on Density Functional Theory (DFT) provide valuable insights into the electronic properties and charge distribution of BMI. The atomic charges (Figure 7) obtained from the DFT calculations offer crucial information about the distribution of electron density within the molecular structure, which has significant implications for understanding the corrosion inhibition mechanism [65, 66].

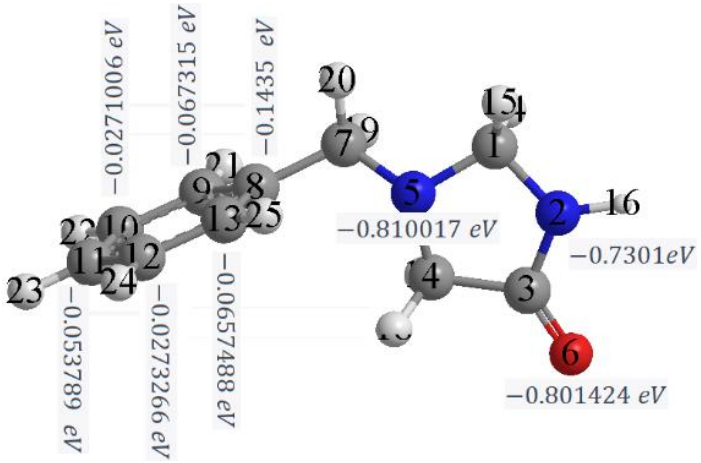

Figure 7. The DFT calculations revealed the atomic charges for specific atoms in BMI.

The variation in atomic charges reflects the different electronic environments and bonding characteristics of the atoms in the molecular structure. The presence of nitrogen atoms N(2) and N(5) with negative charges indicates that these atoms are electron-rich and have the potential to act as electron donors. The lone pairs of electrons on the nitrogen atoms make them suitable sites for forming coordination bonds with metal ions on the mild steel surface. This ability to donate electrons enhances the inhibitor's adsorption and inhibitory behavior. Additionally, the presence of oxygen atoms O(6) with negative charges suggests that they can also participate in charge transfer processes. Oxygen atoms are known for their ability to form strong interactions with metal ions, contributing to the formation of protective films on the metal surface [67, 68]. Furthermore, the aromatic carbon atoms C(8), C(9), C(10), C(11), C(12) and C(13) have slightly negative charges, indicating that they are also electron-rich. The delocalized π-electron cloud in the aromatic ring system enhances the electronic interactions between the inhibitor and the metal surface. The aromatic carbon atoms play a significant role in establishing Van der Waals forces and π–π interactions with metal atoms, further stabilizing the inhibitor-metal surface interface. The knowledge of atomic charges obtained from DFT calculations is essential for understanding the nature of bonding interactions between the inhibitor and the metal surface. The negatively charged nitrogen and oxygen atoms facilitate the formation of strong coordination bonds, while the aromatic carbon atoms contribute to additional interactions, such as Van der Waals forces

and π–π interactions. Overall, the DFT calculations and atomic charges provide valuable insights into the electronic structure and charge distribution of BMI [69, 70]. The electron-rich nature of specific atoms in the inhibitor molecule enhances its interaction with the metal surface, leading to effective corrosion inhibition. The combination of experimental and theoretical approaches contributes to a comprehensive understanding of the inhibitory mechanism, supporting the potential application of BMI as a corrosion inhibitor for mild steel in aggressive environments.

3.4. Suggested inhibition mechanism

The experimental and theoretical investigations provide valuable insights into the corrosion inhibition mechanism of BMI on mild steel in a 1 M HCl solution. The adsorption behavior observed through adsorption isotherm analysis points towards a combination of chemical and physical adsorption as the primary inhibition mechanism [71, 72]. Chemical adsorption involves strong and specific interactions between the inhibitor molecules and the metal surface. In this case, the presence of nitrogen atoms in the heterocyclic imidazolidinone ring of the inhibitor plays a crucial role [73, 74]. The lone pairs of electrons on the nitrogen atoms act as donor sites, and they can interact with vacant d-orbitals of iron ions present on the metal surface (Figure 8). These interactions are predominantly of a covalent nature, resulting in the formation of stable coordination bonds between the inhibitor and the metal. The vacant d-orbitals of iron ions on the metal surface act as acceptor sites, facilitating the sharing or transfer of electrons with the inhibitor molecules. This leads to the establishment of strong metal-inhibitor bonds, contributing to the formation of a protective film on the mild steel surface. In addition to chemical adsorption, physical adsorption also plays a role in the corrosion inhibition mechanism. Physical adsorption is characterized by weaker forces, such as Van der Waals forces and electrostatic interactions, between the inhibitor and the metal surface (Figure 8). While these interactions are not as strong as chemical bonds, they still contribute to the overall adsorption process [75].

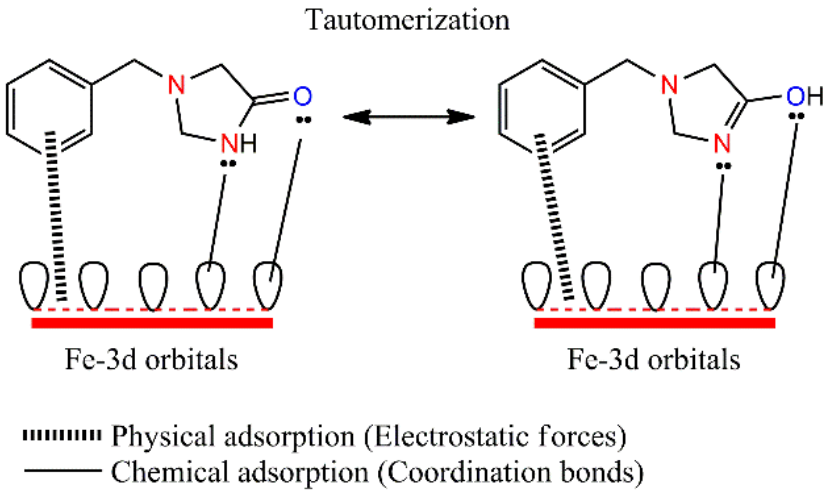

Figure 8. Suggested inhibition mechanism.

The presence of heterocyclic imidazolidinone in the inhibitor's molecular structure enhances the physical adsorption. The aromatic ring system in imidazolidinone provides a delocalized electron cloud, which can interact with the metal surface through Van der Waals forces. These interactions, combined with the chemical bonding, further stabilize the inhibitor film on the metal surface [76]. Overall, the suggested inhibition mechanism involves a combination of chemical adsorption, facilitated by the presence of nitrogen atoms in the heterocyclic imidazolidinone ring, and physical adsorption, enhanced by the aromatic nature of the inhibitor's structure. The interactions between the inhibitor molecules and the metal surface, particularly with the vacant d-orbitals of iron ions, play a pivotal role in the formation of a protective layer on the mild steel surface. This dual mechanism of adsorption enables BMI to effectively hinder the corrosive attack of hydrochloric acid on mild steel. The strong chemical bonds provide a stable and permanent barrier, while the weaker physical interactions contribute to the overall stability and coverage of the protective film [1, 23, 27]. The comprehensive understanding of the suggested inhibition mechanism is essential for designing effective corrosion inhibitors and optimizing their performance in practical industrial applications. The insights gained from this study lay the foundation for further development and exploration of corrosion protection strategies using organic inhibitors derived from imidazole for various metal substrates in aggressive environments [77].

4. Conclusion

In conclusion, this research study explored the corrosion inhibition potential of BMI for mild steel in a 1 M hydrochloric acid (HCl) solution. Through a combined approach involving weight loss measurements and quantum chemical calculations using Density Functional Theory (DFT), the inhibition efficiency and adsorption behavior of the inhibitor on the metal surface were thoroughly investigated. The experimental results demonstrated that BMI exhibited remarkable corrosion inhibition properties, with an impressive inhibition efficiency of 94.8% at an inhibitor concentration of 0.5 mM in 1 M HCl for a 5-hour immersion period at 303 K. The inhibition efficiency increased with increasing immersion time up to 10 hours, beyond which it slightly decreased at 24 hours. However, even at extended immersion periods, the inhibitor continued to provide significant corrosion protection for mild steel.

Moreover, the investigation of the effect of inhibitor concentrations revealed that higher concentrations led to stronger adsorption of the inhibitor on the metal surface, resulting in enhanced corrosion inhibition efficiency. The Langmuir adsorption isotherm model provided a good fit to the experimental data, indicating that BMI formed a complete and stable monolayer on the metal surface, hindering further corrosive attacks. Additionally, the analysis of the effect of temperature showed that the inhibition efficiency of the inhibitor decreased slightly with increasing temperature. Nonetheless, even at elevated temperatures, BMI demonstrated significant corrosion protection, underscoring its potential for application in diverse temperature conditions. The adsorption isotherm analysis further shed light on the

adsorption behavior of the inhibitor on the mild steel surface. The Langmuir isotherm accurately described the adsorption process, with a high *R*-squared value of 0.99506, suggesting a spontaneous and favorable adsorption mechanism. The negative standard free energy of adsorption $\left(\Delta G^0_{ads}\right)$ of –35.68 kJ·mol^{-1} indicated chemisorption, involving strong and covalent bonding between the inhibitor and the metal surface. The suggested inhibition mechanism involved a combination of chemical and physical adsorption. The presence of nitrogen atoms in the heterocyclic imidazolidinone ring facilitated the formation of strong metal-inhibitor bonds through interactions with vacant d-orbitals of iron ions on the metal surface. Additionally, physical interactions, such as Van der Waals forces and electrostatic interactions, further stabilized the inhibitor film on the mild steel surface.

Overall, BMI exhibited promising potential as an efficient and environmentally friendly corrosion inhibitor for mild steel in acidic environments. The synergistic insights gained from the experimental and theoretical approaches provided a comprehensive understanding of the corrosion inhibition process, paving the way for practical industrial applications. The findings of this research contribute to the advancement of corrosion protection strategies, offering opportunities for the development of novel organic inhibitors derived from imidazole for various metal substrates in aggressive environments. In conclusion, the results of this study highlight the significance of BMI as a promising corrosion inhibitor and provide valuable insights into its inhibition mechanism. This research opens avenues for further investigations and optimizations in the field of corrosion inhibition, with potential implications for enhancing the lifespan and durability of metallic materials in industrial applications.

References

1. A.M. Resen, M. Hanoon, R.D. Salim, A.A. Al-Amiery, L.M. Shaker and A.A.H. Kadhum, Gravimetrical, theoretical, and surface morphological investigations of corrosion inhibition effect of 4-(benzoimidazole-2-yl) pyridine on mild steel in hydrochloric acid, *Koroze Ochr. Mater*., 2020, **64**, 122–130. doi: 10.2478/kom-2020-0018
2. M.M. Solomon, I.E. Uzoma, J.A.O. Olugbuyiro and O.T. Ademosun, A censorious appraisal of the oil well acidizing corrosion inhibitors, *J. Pet. Sci. Eng*., 2022, **215**, 110711. doi: 10.1016/j.petrol.2022.110711 2
3. B.D.B. Tiu and R.C. Advincula, Polymeric corrosion inhibitors for the oil and gas industry: design principles and mechanism, *React. Funct. Polym*., 2015, **95**, 25–45. doi: 10.1016/j.reactfunctpolym.2015.08.006
4. F.F.S. Firas, S.I. Ibrahim, M.M. Hanoon, A.A.H. Kadhum and A.A. Al-amiery, Gravimetric measurements and theoretical calculations of 4-aminoantipyrine derivatives as corrosion inhibitors for mild steel in hydrochloric acid solution: comparative studies, *Corros. Sci. Technol*., 2023, **22**, no. 2, 73–89.

5. M. Farsak, H. Keleş and M.A. Keleş, New corrosion inhibitor for protection of low carbon steel in HCl solution, *Corros. Sci*., 2015, **98**, 223–232. doi: 10.1016/j.corsci.2015.05.036
6. A. Alamiery, W.N.R.W. Isahak, H.S.S. Aljibori, H.A. Al-Asadi and A.A.H. Kadhum, Effect of the structure, immersion time and temperature on the corrosion inhibition of 4-pyrrol-1-yl-*n*-(2,5-dimethyl-pyrrol-1-yl)benzoylamine in 1.0 M HCl solution, *Int. J. Corros. Scale Inhib*., 2021, **10**, no. 2, 700–713. doi: 10.17675/2305-6894-2021-10-2-14
7. B.S. Mahdi, M.K. Abbass, M.K. Mohsin, W.K. Al-Azzawi, M.M. Hanoon, M.H.H. AlKaabi, L.M. Shaker, A.A. Al-Amiery, W.N.R.W. Isahak, A.A.H. Kadhum and M.S. Takriff, Corrosion inhibition of mild steel in hydrochloric acid environment using terephthaldehyde based on Schiff base: gravimetric, thermodynamic, and computational studies, *Molecules*, 2022, **27**, no. 15, 4857. doi: 10.3390/molecules27154857
8. A.H. Alamri, Localized corrosion and mitigation approach of steel materials used in oil and gas pipelines – An Overview, *Eng. Failure Anal*., 2020, **116**, 104735. doi: 10.1016/j.engfailanal.2020.104735
9. D. Jeroundi, S. Chakroune, H. Elmsellem, E.M.El Hadrami, A. Ben-Tama, A. Elyoussfi, A. Dafali, C. Douez and B. Hafez, 2,3-(2-alkylthio)-6,7-bis(2-alkylthio)TTF: a new and green synthetic anti-corrosive inhibitors for mild steel in 1.0 HCl, *J. Mater. Environ. Sci*., 2018, **9**, no. 1, 334–344. doi: 10.26872/jmes.2018.9.1.37
10. M.H. Mahross, K. Efil, T.A. Seif El-Nasr and O.A. Abbas, Experimental and theoretical study on corrosion inhibition of mild steel in oilfield formation water using some schiff base metal complexes, *J. Electrochem. Sci. Technol*., 2017, **8**, no. 3, 222–235. doi: 10.5229/JECST.2017.8.3.222
11. I.B. Obot, D.D. Macdonald and Z.M. Gasem, Density functional theory (DFT) as a powerful tool for designing new organic corrosion inhibitors. Part 1: An overview, *Corros. Sci*., 2015, **99**, 1–30. doi: 10.1016/j.corsci.2015.01.037
12. M. Filali, E.M. El Hadrami, A. Ben-tama, B. Hafez, I. Abdel-Rahman, A. Harrach, H. Elmsellem, B. Hammouti, M. Mokhtari, S.E. Stiriba and M. Julve, 3,6-di(pyridin-2-yl) pyridazine derivatives as original and new corrosion inhibitors in support of mild steel: experimental studies and DFT investigational, *Int. J. Corros. Scale Inhib*., 2019, **8**, no. 1, 93–109. doi: 10.17675/2305-6894-2019-8-1-9
13. D.S. Chauhan, M.A.J. Mazumder, M.A. Quraishi and K.R. Ansari, Chitosan cinnamaldehyde Schiff base: A bioinspired macromolecule as corrosion inhibitor for oil and gas industry, *Int. J. Biol. Macromol*., 2020, **158**, 127–138. doi: 10.1016/j.ijbiomac.2020.04.200
14. S. Şafak, B. Duran, A. Yurt and G. Türkoğlu, Schiff bases as corrosion inhibitor for aluminium in HCl solution, *Corros. Sci*., 2012, **54**, 251–259. doi: 10.1016/j.corsci.2011.09.026

15. H.S. Aljibori, A.H. Alwazir, S. Abdulhadi, W.K. Al-Azzawi, A.A.H. Kadhum, L.M. Shaker, A.A. Al-Amiery and H.Sh. Majdi, The use of a Schiff base derivative to inhibit mild steel corrosion in 1 M HCl solution: a comparison of practical and theoretical findings, *Int. J. Corros. Scale Inhib*., 2022, **11**, no. 4, 1435–1455. doi: 10.17675/2305- 6894-2022-11-4-2
16. A. Mustafa, F. Sayyid, N. Betti, M. Hanoon, A. Al-Amiery, A. Kadhum and M. Takriff, Inhibition evaluation of 5-(4-(1*H*-pyrrol-1-yl)phenyl)-2-mercapto-1,3,4-oxadiazole for the corrosion of mild steel in an acid environment: Thermodynamic and DFT aspects, *Tribologia*, 2021, **38**, 39–47. doi: 10.30678/fjt.105330
17. M.S. Abdulazeez, Z.S. Abdullahe, M.A. Dawood, Z.K. Handel, R.I. Mahmood, S. Osamah, A.H. Kadhum, L.M. Shaker and A.A. Al-Amiery, Corrosion inhibition of low carbon steel in HCl medium using a thiadiazole derivative: weight loss, DFT studies and antibacterial studies, *Int. J. Corros. Scale Inhib*., 2021, **10**, no. 4, 1812–1828. doi: 10.17675/2305-6894-2021-10-4-27
18. K.M. Manamela, L.C. Murulana, M.M. Kabanda and E.E. Ebenso, Adsorptive and DFT studies of some imidazolium based ionic liquids as corrosion inhibitors for zinc in acidic medium, *Int. J. Electrochem. Sci*., 2014, **9**, 3029–3046.
19. M. Yadav, S. Kumar, R.R. Sinha, I. Bahadur and E.E. Ebenso, New pyrimidine derivatives as efficient organic inhibitors on mild steel corrosion in acidic medium: electrochemical, SEM, EDX, AFM and DFT studies, *J. Mol. Liq*., 2015, **211**, 135–145. doi: 10.1016/j.molliq.2015.06.063
20. G. Gao and C. Liang, Electrochemical and DFT studies of β-amino-alcohols as corrosion inhibitors for brass, *Electrochim. Acta*, 2007, **52**, 4554–4559. doi: 10.1016/j.electacta.2006.12.058
21. Al-Amiery and M.S. Takriff, Exploration of 8-piperazine-1-ylmethylumbelliferone for application as a corrosion inhibitor for mild steel in hydrochloric acid solution, *Int. J. Corros. Scale Inhib*., 2021, **10**, no. 1, 368–387. doi: 10.17675/2305-6894-2021-10-1-21
22. M.M. Hanoon, A.M. Resen, A.A. Al-Amiery, A.A.H. Kadhum and M.S. Takriff, Theoretical and experimental studies on the corrosion inhibition potentials of 2-((6-methyl-2-ketoquinolin-3-yl) methylene) hydrazinecarbothioamide for mild steel in 1 M HCl, *Prog. Color, Color. Coat*., 2022, **15**, 11–23. doi: 10.30509/PCCC.2020.166739.1095
23. Y.M. Abdulsahib, A.J.M. Eltmimi, S.A. Alhabeeb, M.M. Hanoon, A.A. Al-Amiery, T. Allami and A.A.H. Kadhum, Experimental and theoretical investigations on the inhibition efficiency of *N*-(2,4-dihydroxytolueneylidene)-4-methylpyridin-2-amine for the corrosion of mild steel in hydrochloric acid, *Int. J. Corros. Scale Inhib*., 2021, **10**, no. 3, 885–899. doi: 10.17675/2305-6894-2021-10-3-3
24. A.K. Khudhair, A.M. Mustafa, M.M. Hanoon, A. Al-Amiery, L.M. Shaker, T. Gazz, A.B. Mohamad, A.H. Kadhum and M.S. Takriff, Experimental and theoretical investigation on the corrosion inhibitor potential of *N*-MEH for Mild Steel in HCl, *Prog. Color, Color. Coat*., 2022, **15**, 111–122. doi: 10.30509/PCCC.2021.166815.1111

25. D.S. Zinad, R.D. Salim, N. Betti, L.M. Shaker and A.A. AL-Amiery, Comparative investigations of the corrosion inhibition efficiency of a 1-phenyl-2-(1-phenylethylidene)hydrazine and its analog against mild steel corrosion in hydrochloric acid solution, *Prog. Color, Color. Coat.*, 2022, **15**, 53–63. doi: 10.30509/pccc.2021.166786.1108
26. A.Z. Salman, Q.A. Jawad, K.S. Ridah, L.M. Shaker and A.A. Al-Amiery, Selected bis-thiadiazole: synthesis and corrosion inhibition studies on mild steel in HCl environment, *Surf. Rev. Lett.*, 2020, **27**, 2050014. doi: 10.1142/S0218625X20500146
27. ASTM International, *Standard Practice for Preparing, Cleaning, and Evaluating Corrosion Test*, 2011, 1–9.
28. NACE International, *Laboratory corrosion testing of metals in static chemical cleaning solutions at temperatures below 93°C (200°F)*, TM0193-2016-SG, 2000.
29. M.J. Frisch, G.W. Trucks, H.B. Schlegel, G.E. Scuseria, M.A. Robb, J.R. Cheeseman, J.A. Montgomery, T. Vreven, K.N. Kudin, J.C. Burant, J.M. Millam, S.S. Iyengar, J. Tomasi, V. Barone, B. Mennucci, M. Cossi, G. Scalmani, N. Rega, G.A. Petersson, H. Nakatsuji, M. Hada, M. Ehara, K. Toyota, R. Fukuda, J. Hasegawa, M. Ishida, T. Nakajima, Y. Honda, O. Kitao, H. Nakai, M. Klene, X. Li, J.E. Knox, H.P. Hratchian, J.B. Cross, V. Bakken, C. Adamo, J. Jaramillo, R. Gomperts, R.E. Stratmann, O. Yazyev, A.J. Austin, R. Cammi, C. Pomelli, J.W. Ochterski, P.Y. Ayala, K. Morokuma, G.A. Voth, P. Salvador, J.J. Dannenberg, V.G. Zakrzewski, S. Dapprich, A.D. Daniels, M.C. Strain, O. Farkas, D.K. Malick, A.D. Rabuck, K. Raghavachari, J.B. Foresman, J.V. Ortiz, Q. Cui, A.G. Baboul, S. Clifford, J. Cioslowski, B.B. Stefanov, G. Liu, A. Liashenko, P. Piskorz, I. Komaromi, R.L. Martin, D.J. Fox, T. Keith, M.A. Al-Laham, C.Y. Peng, A. Nanayakkara, M. Challacombe, P.M.W. Gill, B. Johnson, W. Chen, M.W. Wong, C. Gonzalez and J.A. Pople, *Gaussian 03, Revision B. 05*, Gaussian, Inc., Wallingford, CT, 2004.
30. T. Koopmans, Ordering of wave functions and eigen-energies to the individual electrons of an atom, *Physica*, 1934, **1**, no. 1–6, 104–113 (in German). doi: 10.1016/S0031-8914(34)90011-2
31. W.K. Al-Azzawi, A.J. Al Adily, F.F. Sayyid, R.K. Al-Azzawi, M.H. Kzar, H.N. Jawoosh, A.A. Al-Amiery, A.A.H. Kadhum, W.N.R.W. Isahak and M.S. Takriff, Evaluation of corrosion inhibition characteristics of an *N*-propionanilide derivative for mild steel in 1 M HCl: Gravimetrical and computational studies, *Int. J. Corros. Scale Inhib.*, 2022, **11**, no. 3, 1100–1114. doi: 10.17675/2305-6894-2022-11-3-12
32. R.D. Salim, N. Betti, M. Hanoon and A.A. Al-Amiery, 2-(2,4-Dimethoxybenzylidene)-*N*-Phenylhydrazinecarbothioamide as an Efficient Corrosion Inhibitor for Mild Steel in Acidic Environment, *Prog. Color, Color. Coat.*, 2021, **15**, 45–52. doi: 10.30509/pccc.2021.166775.1105

33. A.A. Al-Amiery, L.M. Shaker, A.H. Kadhum and M.S. Takriff, Exploration of furan derivative for application as corrosion inhibitor for mild steel in hydrochloric acid solution: Effect of immersion time and temperature on efficiency, *Mater. Today: Proc*., 2021, **42**, 2968–2973. doi: 10.1016/j.matpr.2020.12.807
34. A.A. Al-Amiery, W.N.R.W. Isahak and W.K. Al-Azzawi, Corrosion Inhibitors: Natural and Synthetic Organic Inhibitors, *Lubricants*, 2023, **11**, 174. doi: 10.3390/lubricants11040174
35. M.K. Abbass, K.M. Raheef, I.A. Aziz, M.M. Hanoon, A.M. Mustafa, W.K. Al-Azzawi, A.A. Al-Amiery and A.A.H. Kadhum, Evaluation of 2-Dimethylaminopropionamido-antipyrine as a Corrosion Inhibitor for Mild Steel in HCl Solution: A Combined Experimental and Theoretical Study, *Prog. Color, Color. Coat*., 2024, **17**, no. 1, 1–10. doi: 10.30509/pccc.2023.167081.1197
36. P. Muthukrishnan, B. Jeyaprabha, P. Prakash, Adsorption and corrosion inhibiting behavior of Lannea coromandelica leaf extract on mild steel corrosion, *Arab. J. Chem*., 2017, **10**, S2343–S2354, doi: 10.1016/j.arabjc.2013.08.011
37. B. Hammouti, A. Zarrouk, S.S. Al-Deyab and I. Warad, Temperature effect, activation energies and thermodynamics of adsorption of ethyl 2-(4-(2-ethoxy-2-oxoethyl)-2-ptolylquinoxalin-1(4h)-yl) acetate on Cu in HNO_3, *Orient. J. Chem*., 2011, **27**, no. 1, 23–31.
38. E.A. Noor and A.H. Al-Moubaraki, Thermodynamic study of metal corrosion and inhibitor adsorption processes in mild steel/1-methyl-4[4'-(-*X*)-styryl pyridinium iodides/hydrochloric acid systems, *Mater. Chem. Phys*., 2008, **110**, 145–154. doi: 10.1016/j.matchemphys.2008.01.028
39. O. Benali, L. Larabi, M. Traisnel, L. Gengembre and Y. Harek, Electrochemical, theoretical and XPS studies of 2-mercapto-1-methylimidazole adsorption on carbon steel in 1 M $HClO_4$, *Appl. Surf. Sci*., 2007, **253**, no. 14, 6130–6139. doi: 10.1016/j.apsusc.2007.01.075
40. R. Haldhar, D. Prasad, A. Saxena, P. Singh, valeriana wallichii root extract as a green & sustainable corrosion inhibitor for mild steel in acidic environments: experimental and theoretical, *Mater. Chem. Front*., 2018, **2**, 1225–1237. doi: 10.1039/C8QM00120K
41. L.O. Olasunkanmi, I.B. Obot, M.M. Kabanda and E.E. Ebenso, Some quinoxalin-6-yl derivatives as corrosion inhibitors for mild steel in hydrochloric acid: experimental and theoretical studies, *J. Phys. Chem. C*, 2015, **119**, 16004–16019.
42. M. Stern and A.L. Geary, Electrochemical polarization, I. theoretical analysis of the shape of polarisation curves, *J. Electrochem. Soc*., 1957, **104**, 56–63. doi: 10.1149/1.2428496
43. M.A. Amin, M.A. Ahmed, H.A. Arida, F. Kandemirli, M. Saracoglu, T. Arslan and M.A. Basaran, Monitoring corrosion and corrosion control of iron in HCl by non-ionic surfactants of the TRITON-X series–part III. Immersion time effects and theoretical studies, *Corros. Sci*., 2011, **53**, 1895–1909. doi: 10.1016/j.corsci.2011.02.007

44. K.F. Khaled and M.M. Al-Qahtani, The Inhibitive effect of some DETS Crazole derivatives towards Al corrosion in acid solution: chemical, electrochemical and theoretical studies, *Mater. Chem. Phys*., 2009, **113**, 150–158. doi: 10.1016/j.matchemphys.2008.07.060
45. D. Ben Hmamou, R. Salghi, A. Zarrouk, H. Zarrok, R. Touzani, B. Hammouti and A. El Assyry, Investigation of corrosion inhibition of carbon steel in 0.5 M H_2SO_4 by new bipyrazole derivative using experimental and theoretical approaches, *J. Environ. Chem. Eng*., 2015, **3**, 2031–2041. doi: 10.1016/j.jece.2015.03.018
46. H. Ma, S. Chen, Z. Liu and Y. Sun, Theoretical elucidation on the inhibition mechanism of pyridine-pyrazole compound: a Hartree Fock study, *J. Mol. Struct.: THEOCHEM*, 2006, **774**, no. 1–3, 19–22. doi: 10.1016/j.theochem.2006.06.044
47. P. Mourya, P. Singh, A.K. Tewari, R.B. Rastogi and M.M. Singh, Relationship between structure and inhibition behaviour of quinolinium salts for mild steel corrosion: experimental and theoretical approach, *Corros. Sci*., 2015, **95**, 71–87. doi: 10.1016/j.corsci.2015.02.034
48. G. Gece, The use of quantum chemical methods in corrosion inhibitor studies, *Corros. Sci*., 2008, **50**, 2981–2992. doi: 10.1016/j.corsci.2008.08.043
49. V.S. Sastri and J.R. Perumareddi, Molecular orbital theoretical studies of some organic corrosion inhibitors, *Corrosion*, 1997, **53**, 617–622. doi: 10.5006/1.3290294
50. S. Hadisaputra, A.A. Purwoko, I. Ilhamsyah, S. Hamdiani, D. Suhendra, N. Nuryono and B. Bundjali, A combined experimental and theoretical study of (*E*)-ethyl 3-(4-methoxyphenyl)acrylate as corrosion inhibitor of iron in 1 M HCl solutions, *Int. J. Corros. Scale Inhib*., 2018, **7**, no. 4, 633–647. doi: 10.17675/2305-6894-2018-7-4-10
51. M. Lagrenée, B. Mernari, M. Bouanis, M. Traisnel and F. Bentiss, Study of the mechanism and inhibiting efficiency of 3,5-bis(4-methylthiophenyl)-4*H*-1,2,4-triazole on mild steel corrosion in acidic media, *Corros. Sci*., 2002, **44**, no. 3, 573–588. doi: 10.1016/S0010-938X(01)00075-0
52. G. Quartarone, M. Battilana, L. Bonaldo and T. Tortato, Investigation of the inhibition effect of indole-3-carboxylic acid on the copper corrosion in 0.5 M H_2SO_4, *Corros. Sci*., 2008, **50**, 3467–3474. doi: 10.1016/j.corsci.2008.09.032
53. A. Döner and G. Kardaş, *N*-Aminorhodanine as an effective corrosion inhibitor for mild steel in 0.5 M H_2SO_4, *Corros. Sci*., 2011, **53**, 4223–4232. doi: 10.1016/j.corsci.2011.08.032
54. A. El Yaktini, A. Lachiri, M. El Faydy, F. Benhiba, H. Zarrok, M. El Azzouzi, M. Zertoubi, M. Azzi, B. Lakhrissi and A. Zarrouk. Inhibitor effect of new azomethine derivative containing an 8-hydroxyquinoline moiety on corrosion behavior of mild carbon steel in acidic media, *Int. J. Corros. Scale Inhib*., 2018, **7**, no. 4, 609–632. doi: 10.17675/2305-6894-2018-7-4-9
55. H. Ma, S. Chen, Z. Liu and Y. Sun, Theoretical elucidation on the inhibition mechanism of pyridine-pyrazole compound: a Hartree Fock study, *J. Mol. Struct.: THEOCHEM*, 2006, **774**, no. 1–3, 19–22. doi: 10.1016/j.theochem.2006.06.044

56. M.F. Chiter, Theoretical study of green corrosion inhibitors: adsorption of 8-hydroxquinoline on aluminum surface, National polytechnic institute of Toulouse, University of Toulouse, Toulouse, France, 2015.
57. S. Kaya and C. Kaya, A new equation for calculation of chemical hardness of groups and molecules, *Mol. Phys*., 2015, **113**, no. 11, 1311–1319. doi: 10.1080/00268976.2014.991771
58. S. Kaya and C. Kaya, A new method for calculation of molecular hardness: a theoretical study, *Comput. Theor. Chem*., 2015, **1060**, 66–70. doi: 10.1016/j.comptc.2015.03.004
59. S. Kaya and C. Kaya, A simple method for the calculation of lattice energies of inorganic ionic crystals based on the chemical hardness, *Inorg. Chem*., 2015, **54**, no. 17, 8207–8213. doi: 10.1021/acs.inorgchem.5b00383
60. S. Kaya, C. Kaya and N. Islam, Maximum hardness and minimum polarizability principles through lattice energies of ionic compounds, *Phys. B*, 2016, **485**, 60–66. doi: 10.1016/j.physb.2016.01.010
61. K. Khaled, Studies of iron corrosion inhibition using chemical, electrochemical and computer simulation techniques, *Electrochim. Acta*, 2010, **55**, no. 22, 6523–6532. doi: 10.1016/j.electacta. 2010.06.027
62. H. Elmsellem, H. Nacer, F. Halaimia, A. Aouniti, I. Lakehal, A. Chetouani and B. Hammouti, Anti-corrosive Properties and Quantum Chemical Study of (E)-4-Methoxy-N-(Methoxybenzylidene)Aniline and (E)-N-(4-Methoxybenzylidene)-4-Nitroaniline Coating on Mild Steel in Molar Hydrochloric, *Int. J. Electrochem. Sci*., 2014, **9**, 5328–5351.
63. A.T. Hassan, R.K. Hussein, M. Abou-Krisha and M.I. Attia, Density functional theory investigation of some pyridine dicarboxylic acids derivatives as corrosion inhibitors, *Int. J. Electrochem. Sci*., 2020, **15**, 4274–4286. doi: 10.20964/2020.05.11
64. B. Tüzün and C. Kaya, Investigation of DNA–RNA Molecules for the efficiency and activity of corrosion inhibition by DFT and molecular docking, *J. Bio Tribo Corros*., 2018, **4**. doi: 10.1007/s40735-018-0185-5
65. S. Erdogan and B. Tüzün, Applications of the effectiveness of corrosion inhibitors with computational methods and molecular dynamics simulation, in: applications of the effectiveness of corrosion inhibitors with computational methods and molecular dynamics simulation, *Corrosion*, 2021. doi: 10.5772/intechopen.98968
66. K.F. Khaled and M.M. Al-Qahtani, The inhibitive effect of some tetrazole derivatives towards Al corrosion in acid solution: chemical, electrochemical and theoretical studies, *Mater. Chem. Phys*., 2009, **113**, no. 1, 150–158. doi: 10.1016/j.matchemphys.2008.07.060
67. I. Lukovits, E. Kalman and F. Zucchi, Corrosion inhibitors: correlation between electronic structure and efficiency, *Corrosion*, 2001, **57**, no. 1, 3–8. doi: 10.5006/1.3290328

68. A. Shaban, I. Felhosi and J. Telegdi, Laboratory assessment of inhibition efficiency and mechanism of inhibitor blend (P22SU) on mild steel corrosion in high chloride containing water, *Int. J. Corros. Scale Inhib*., 2017, **6**, no. 3, 262–275. doi: 10.17675/2305-6894-2017-6-3-3
69. I. Obot, N. Obi-Egbedi and A. Eseola, Anticorrosion Potential of 2-Mesityl-1H-imidazo[4,5-f][1,10]phenanthroline on Mild Steel in Sulfuric Acid Solution: Experimental and Theoretical Study, *Ind. Eng. Chem. Res*., 2011, **50**, no. 4, 2098–2110. doi: 10.1021/ie102034c
70. D.K. Yadav and M. Quraishi, Electrochemical investigation of Substituted Pyranopyrazoles Adsorption on Mild Steel in Acid Solution, *Ind. Eng. Chem. Res*., 2012, **51**, no. 24, 8194–8210. doi: 10.1021/ie3002155
71. A. Ostovari, S. Hoseinieh, M. Peikari, S. Shadizadeh and S. Hashemi, Corrosion inhibition of mild steel in 1 M HCl solution by henna extract: A comparative study of the inhibition by henna and its constituents (Lawsone, Gallic acid, α-d-Glucose and Tannic acid), *Corros. Sci*., 2009, **51**, no. 9, 1935–1949. doi: 10.1016/j.corsci.2009.05.024
72. M. El-Naggar, Corrosion inhibition of mild steel in acidic medium by some sulfa drugs compounds, *Corros. Sci*., 2007, **49**, no. 5, 2226–2236. doi: 10.1016/j.corsci.2006.10.039
73. C.B. Verma, M. Quraishi and A. Singh, J. Taiwan, *Inst. Chem. Eng*., 2015, **49**, 229–239.
74. C. Verma, E.E. Ebenso and M.A. Quraishi, Alkaloids as green and environmental benign corrosion inhibitors: An overview, *Int. J. Corros. Scale Inhib*., 2019, **8**, no. 3, 512–528. doi: 10.17675/2305-6894-2019-8-3-3
75. A.S. Fouda, H.M. El-Abbasy and A.A. El-Sherbini, Inhibitive effect of artemisia judaica herbs extract on the corrosion of carbon steel in hydrochloric acid solutions, *Int. J. Corros. Scale Inhib*., 2018, **7**, no. 2, 213–235. doi: 10.17675/2305-6894-2018-7-2-8
76. S. Hadisaputra, A.A. Purwoko, F. Wajdi, I. Sumarlan and S. Hamdiani, Theoretical study of the substituent effect on corrosion inhibition performance of benzimidazole and its derivatives, *Int. J. Corros. Scale Inhib*., 2019, **8**, no. 3, 673–688. doi: 10.17675/2305-6894-2019-8-3-15
77. S. Martinez, Inhibitory mechanism of mimosa tannin using molecular modeling and substitutional adsorption isotherms, *Mater. Chem. Phys*., 2002, **77**, no. 1, 97–102. doi: 10.1016/S0254-0584(01)00569-7

♦ ♦ ♦